The Molecular Mechanism and Potential Dependence of the Na^+/Glucose Cotransporter

Eric Bennett and George A. Kimmich
Departments of Biophysics and Biochemistry, University of Rochester School of Medicine and Dentistry, Rochester, New York 14642 USA

ABSTRACT Activity of the Na^+/glucose cotransporter endogenously expressed in LLC-PK_1 cells was measured using whole cell recording techniques under three different sodium concentration conditions: 1) externally saturating, zero trans; 2) 40 mM external, zero trans; and 3) externally saturating, 50 mM trans. Activity of the transporter with increasing concentrations of sugar was measured for each set of conditions, from which the maximal current for saturating sugar, I_m, was determined. The I_m measured shows substantial potential dependence for each set of conditions. The absolute I_m and the relative potential dependence of I_m compared among the various solute conditions were used to identify which loci in the transport cycle are responsible for potential-dependent changes in function. The experimental data were compared with the predicted I_m values calculated from an eight-state, sequential, reversible model of a transport reaction kinetic scheme. Predictions derived from assignment of rate limitation and/or potential dependence to each of the 16 transitions in the transport pathway were derived and compared with the measured data. Most putative models were dismissed because of lack of agreement with the measured data, indicating that several steps along the transport pathway are not rate limiting and/or not potential dependent. Only two models were found that can completely account for the measured data. In one case, translocation of the free carrier must be rate limiting, and both extracellular sodium-binding events as well as translocation of both free and fully loaded carrier forms must be potential-dependent transitions. In the second case, translocation of the free carrier and dissociation of the first sodium to be released intracellularly must be equivalently rate limiting. In this case only the two translocation events are required to be potential dependent. The two external sodium-binding events might still be potential dependent, but this is not required to fit the data. Previous reports suggest that the first model is correct; however, no direct experimental data compel us to dismiss the second option as a feasible model.

INTRODUCTION

The Na^+/glucose cotransporter is one member of a family of sodium-dependent cotransport proteins localized in the apical membranes of intestinal and kidney epithelia. These cotransporters allow for the concentrative accumulation of the cotransported solute in the epithelial cell followed by release at the basolateral boundary down a gradient of chemical potential, resulting in the absorption or resorption of these solutes into the circulatory system (Kimmich, 1990).

The Na^+/glucose cotransporter carries two Na^+ and one glucose molecule per transport cycle. Transfer of glucose into the cell against a gradient of chemical potential is driven by coupled flow of Na^+ down its gradient of electrochemical potential (Kimmich and Randles, 1980). Changes in either Na^+ concentration or in membrane potential directly affect functional activity of the transporter. Two recent reports have directly measured current-voltage relationships for the transport system (Smith-Maxwell et al., 1990; Umbach et al., 1990). These two studies provided initial insight into the role that membrane potentials play in the molecular mechanism of the cotransport protein under conditions in which both elements of the thermodynamic driving force acting on the system could be carefully controlled. Both studies showed that the membrane potential does not "gate" transporter activity in the sense that many ion channels are gated, but instead serves simply as a thermodynamic driving force for which there is no "threshold" value required to allow initiation of function. Changes in membrane potential cause concomitant changes in transporter activity that are consistent with the direction and magnitude of the net sodium electrochemical gradient. Reversal potentials of sugar-induced whole cell currents verified the 2:1 Na^+/glucose stoichiometry of the system that had been determined earlier from measurement of coupled isotope fluxes. These studies also established that the concentration of sodium required for half-maximal flux ($_{na}K_m$) and the maximal transport rate (I_m) are both potential-dependent functions (Bennett and Kimmich, 1992; Parent et al., 1992a,b).

Before the measurement of cotransporter activity by electrophysiological techniques, most efforts to describe potential dependence of the system started with the assumption that "translocation" of one of the carrier forms (i.e., changes in the free or solute loaded transport protein from "inward" to "outward" facing conformational states, or vice versa) is the rate-limiting and potential-dependent event. This idea was based on the intuitive assumption that a change in macromolecular conformation is likely to occur more slowly than those events in the transport cycle relating to

Received for publication 28 September 1995 and in final form 16 January 1996.

Address reprint requests to Dr. Eric Bennett, Department of Physiology, C240, University of Colorado Health Sciences Center, 4200 E. Ninth Ave., Denver, CO 80262. Tel.: 303-270-5561; Fax: 303-270-8110; E-mail: eric.bennett@uchsc.edu.

© 1996 by the Biophysical Society

0006-3495/96/04/1676/13 $2.00

solute binding or dissociation. The potential dependence of translocation was assumed, perhaps largely because of the ease of calculation when only one event is considered to be both potential dependent and rate limiting (Hansen et al., 1981; Heinz and Geck, 1978; Kessler and Semenza, 1983; Samarzija and Fromter, 1982).

Aronson (1978), Restrepo and Kimmich (1985a,b; 1986), and Kimmich and Randles (1988) were among the first to evaluate whether events in the transport cycle other than changes in carrier conformation might also be involved in explaining the potential dependence of the system. The Aronson analysis proved to be ambiguous because the system was assumed to have a 1:1 coupling stoichiometry rather than the 2:1 coupling that was demonstrated subsequently. Restrepo and Kimmich's analysis of a 2:1 coupled model (1985b) showed that potential dependence for Na^+ binding to the transporter at the extracellular side of the membrane could provide a satisfactory fit to the observed potential dependence of Na^+-dependent influx of isotopically labeled sugar (i.e., a "Na^+ well" concept for potential dependence). Later work by the same group (1986) used Na^+ and potential dependence of phlorizin binding/dissociation to deduce that the first Na^+ to bind may have a higher degree of potential dependence than binding of the second Na^+. This raised the possibility that the binding site for the first Na^+ may be relatively "deep" in the membrane such that the ion "feels" the influence of the membrane potential to a greater degree than does the second Na^+, which therefore may be "finding" its binding site closer to the membrane surface. Finally, Kimmich and Randles (1988) showed that the K_m for extracellular sodium ($_{na}K_m$) and the K_i for intracellular Na^+ ($_{na}K_i$) are potential-dependent parameters, possibly indicating that Na^+ is bound and released in a potential-dependent manner at the two sides of the membrane.

All of the above studies suffer certain drawbacks, however. It is particularly difficult to apply conventional isotope flux methodology under conditions where precise control of the thermodynamic driving forces acting on the cotransport system can not be obtained. Furthermore, the $_{na}K_m$ is a complex expression that is not a direct measure of Na^+ dissociation constants. Although $_{na}K_m$ is weighted in terms that include the rate constants for sodium binding/dissociation, it does not discriminate between the two different Na^+ sites, and it includes many rate constants that relate to events in the transport cycle other than Na^+ binding or dissociation. It is not a valid measure of the affinity of the transport protein for sodium at either binding site, and changes in $_{na}K_m$ or $_{na}K_i$ can reflect changes that do not relate at all to Na^+ binding/dissociation events.

More direct evidence for potential-dependent ion binding was described by Bennett and Kimmich (1992) using whole cell recording techniques. They studied the influence of changes in membrane potential on the maximal rate of transporter function under various solute conditions and showed that the binding of sodium to the transporter at the extracellular side of the membrane must be potential dependent if the usual assumption of rate-limiting translocation of the free carrier is maintained. This finding was further supported in a series of two papers by Parent et al. (1992a,b) in which the authors describe a kinetic model for the rabbit ileum sugar cotransporter exogenously expressed in *Xenopus* oocytes. Their data are also consistent with a rate-limiting carrier translocation event and potential-dependent binding of sodium. Together, these reports provide strong evidence for the possibility that sodium binding to the transporter may be potential dependent if the assumption regarding the rate-limiting event is valid.

The model developed and analyzed by Parent et al. (1992a,b) included the assumption that the two sodium-binding events are identical. As mentioned above, most data suggest that this is not accurate. Two separate investigations have shown that binding of phlorizin, a specific inhibitor of the Na^+/sugar cotransporter, is dependent on both Na^+ and the membrane potential, whereas phlorizin dissociation is Na^+ dependent, but potential independent (Aronson, 1978; Restrepo and Kimmich, 1986). Algebraic analysis of the transport kinetics incorporating these facts shows that the two Na^+-binding events are not identical and must thus be modeled as independent steps in the transport cycle (Restrepo and Kimmich, 1986). In this report, we tackle questions relating to whether further insight can be gained by studying the potential dependence of the transport mechanism without the assumption of identical Na^+-binding events. Indeed, this becomes a necessary consideration if one wishes to evaluate further the nature and degree of potential dependence for each ion binding event. This report also examines an endogenously expressing system, thus avoiding possible artifacts associated with heterologous expression systems.

We describe plausible models that can simulate the kinetics and potential dependence of the Na^+/glucose cotransporter. The activity of the cotransporter under three different solute conditions was measured using whole cell recording techniques, and the maximal rate of transporter function at various membrane potentials under each set of conditions was determined. Because the protein can cycle only as fast as its slowest step(s), the maximal rate at which a transporter functions is a direct reflection of events occurring at the rate-limiting step(s) in the cycle. Under known and different solute conditions, rates at specific sites along the transport cycle can be altered by defined amounts. Then, by measuring maximal rates under these different solute conditions, the effect of these manipulations on the potential dependence of the maximal rate can provide evidence for those events in the transport cycle that are potential dependent (see Bennett and Kimmich, 1992, for more details). After measuring the potential dependence of the maximal rate under the three selected solute conditions, various models describing the transport cycle were tested for agreement with the data. For the Na^+/sugar/Na^+ ordered ter ter model defined earlier (Restrepo and Kimmich, 1985a,b, 1986; Bennett and Kimmich, 1992), all possible variations assuming a single rate-limiting step were tested. The validity of

potential-dependent loci was modeled by assigning potential dependence to various loci and then evaluating whether computer-aided fitting for a given model can simulate the experimentally observed characteristics of potential dependence. Additional analysis consisted of evaluating models in which two sites of rate limitation were assigned. All but two models can be discounted because of lack of agreement with the data. In each of the two viable models, translocation of free carrier and fully loaded carrier are both potential-dependent events. In addition, for model 1, translocation of the free carrier from an inward to an outward facing conformational state must be rate limiting, and both extracellular Na^+ binding events are potential dependent. For model 2, only translocations of the free and fully loaded carrier forms must be potential dependent, but a sodium-occluded state exists such that the first sodium dissociation event at the intracellular side of the membrane is rate limiting in addition to translocation of the free carrier. This model does not exclude the possibility that binding of extracellular Na^+ may also be potential dependent. Data previously reported lend support to model 1, but no direct evidence rules out the second model.

MATERIALS AND METHODS

Cell culture

$LLC\text{-}PK_1$ epithelial cells were grown as monolayer cultures at 37°C in a 5% CO_2 humidified atmosphere as described in detail previously. (Smith-Maxwell et al., 1990; Bennett and Kimmich, 1992). Cultures were grown in an enriched Dulbecco's modified Eagle's medium (DMEM) (Sigma) with 10% fetal bovine serum (Hyclone) added. The medium was changed every 2–3 days. Cells were harvested once a week by incubating them in a calcium/magnesium-free phosphate buffer (CMF-DPBS-EDTA) at 37°C for 40–45 min to induce cell detachment from the plates. The suspended cells were passaged at a 1:10 dilution of the confluent density. Cell stocks were thawed for initial plating at passage 199, and all experiments were performed at passages 208–215.

Cells used in all experiments were plated 7 or 8 days before use, and the medium was changed 1 day before cell harvest. The cells were transferred on the morning of an experiment to glass coverslips at a 1:4 dilution and incubated in DMEM for 3 h before the start of an experiment.

Voltage clamp

All of the hardware and software used are identical to previous reports (Smith-Maxwell et al., 1990; Bennett and Kimmich, 1992). The gigaohm-seal patch-clamp technique of Hamill et al. (1981) was used with a Yale Mk-V patch clamp used to measure currents in a whole cell configuration.

Patch pipettes were made from micropipette glass (Gold Seal Accu-fill 90 Micropipettes). Sylgard 184 (Dow Corning) was used near the tips before fire polishing to reduce pipette capacitance. Tip resistances ranged from 4 to 10 Mohm. An Olympus CK2 inverted microscope was used for observation of cells and electrodes during experimentation.

The major extracellular solution used (155 Na_o^+) contained (in mM): 150 NaCl, 5 KCl, 1 $CaCl_2$, 2 $MgCl_2$, and 10 HEPES; 1 N NaOH was used to titrate the solution to pH 7.35–7.4. Final Na^+ concentration was 155 mM. In the other extracellular solution (40 mM Na^+) 110 mM CsCl replaced an equal amount of NaCl and was titrated to the final pH with CsOH. The major intracellular solution employed (for zero trans experiments) contained (in mM): 130 cesium gluconate, 20 CsCl, 1 $CaCl_2$, 2 $MgCl_2$, 11 ethylene glycol-bis(β-aminoethyl ether)-*N,N,N′,N′*-tetraacetic acid (EGTA), and 10 HEPES. CsOH (5.88 N) was used to titrate the solutions to pH 7.35–7.4, giving a final Cs^+ concentration of 180 mM. In some cases, a 50 mM trans Na^+ solution was used in which 50 mM sodium gluconate was substituted for 50 mM cesium gluconate (50 Na_i^+). Studies using KCl internally instead of CsCl showed no effect on transport activity (data not shown). All solutions were filtered before seal formation using a Gelman (0.2-μm pore) tissue culture-grade filter.

All data were collected at 36–37.5°C using the temperature regulation system described previously (Bennett and Kimmich, 1992). Data collection began at least 5 min after attaining the whole cell configuration to ensure complete dialysis of the intracellular solution. Stable whole cell current reversal potentials indicate that 1 min is sufficient for equilibration of the internal solution.

The holding potential used was −73 mV for the zero trans experiments and −67 mV for the 50 mM trans Na^+ experiments. The difference in holding potential is due to the difference in junction potential of the different solutions. The pulse protocol stepped from the holding potential to a test potential for 100 ms, returning to the holding potential for 400 ms. The range of potentials tested was −133 to −7 mV, with 20-mV steps between test pulses. The data collected were the average of four pulses to any given test potential. Data were collected and solutions were changed as previously described (Smith-Maxwell et al., 1990; Bennett and Kimmich, 1992). Briefly, the currents under pre-α-methylglucoside (AMG) conditions were measured, followed by a 10-ml perfusion of the bath (1.5 ml) with the external solution containing various concentrations of AMG. The temperature of the bath was allowed to reequilibrate after each change in AMG concentration before taking new measurements. As reported earlier, addition of AMG to the bath induces a whole cell current that is completely inhibited by subsequent addition of phlorizin. Phlorizin has no effect in the absence of AMG. The current decrease induced by phlorizin therefore identifies activity of the cotransporter. Steady-state currents were measured both before and after the addition of AMG to the bath, and the sugar-induced current (I_{AMG}) is defined as the difference in whole cell steady-state current between the two conditions. Care was taken to collect data only from cells in which the seal characteristics remained constant throughout the experiment. To allow comparison among cells, I_{AMG} was normalized to cell surface area. The whole cell current was divided by the cell capacitance, giving current values in units of $\mu A/cm^2$. All potentials have been corrected to account for the liquid junction potential (ranging from −4 to −13 mV).

Data analysis and quantification of models

All data were fit to the described equations using Sigmaplot 4.0 (Jandel) to provide the best fit ± SD parameters. Quality of fit of kinetic data and of potential-dependent relationships to the various transport models tested also used Sigmaplot 4.0 curve-fitting capabilities, in which the equations derived in the Appendix to describe the kinetic parameters of the transporter were written into the software. Details of the fits and modeling comparisons are outlined in the Results.

RESULTS

Whole cell, sugar-induced current was measured after the addition of increasing concentrations of external AMG under three different sodium concentration conditions: 1) externally saturated (155 40 Na_o^+), zero trans; 2) 40 mM external, zero trans 50 Na_6^+; and 3) externally saturated, 50 mM trans maximal. From these data, the maximal current at any test membrane potential was determined by fitting the dose-response curve to the Michaelis-Menten function (see Appendix).

The I_m measured for each set of conditions exhibit appreciable potential dependence. Table 1 lists the I_m ± SD at

TABLE 1 Absolute and normalized maximal currents at membrane potentials for each of the three solute conditions studied

Saturated external, zero trans sodium (155 Na_o^+)			Nominal external, zero trans sodium (40 Na_o^+)			Saturated external, nominal internal sodium (50 Na_i^+)		
Membrane potential (mV)	I_m ($-\mu A/cm^2$)	Normalized I_m	Membrane potential (mV)	I_m ($-\mu A/cm^2$)	Normalized I_m	Membrane potential (mV)	I_m ($-\mu A/cm^2$)	Normalized I_m
0	0.734	1.0	0	0.481	1	0	0.585	1
−13	0.89 ± 0.1	1.21 ± 0.14	−13	0.69 ± 0.18	1.43 ± 0.37	−7	0.61 ± 0.04	1.04 ± 0.07
−33	1.1 ± 0.07	1.5 ± 0.1	−33	0.83 ± 0.19	1.73 ± 0.4	−27	0.8 ± 0.06	1.37 ± 0.1
−53	1.24 ± 0.11	1.69 ± 0.15	−53	0.94 ± 0.17	1.95 ± 0.35	−47	0.92 ± 0.07	1.57 ± 0.12
−73	1.36 ± 0.09	1.85 ± 0.12	−73	1.05 ± 0.17	2.18 ± 0.35	−67	1.04 ± 0.08	1.78 ± 0.14
−93	1.57 ± 0.11	2.14 ± 0.15	−93	1.31 ± 0.18	2.72 ± 0.4	−87	1.22 ± 0.08	2.09 ± 0.14
−113	1.79 ± 0.11	2.44 ± 0.15	−113	1.54 ± 0.2	3.2 ± 0.42	−107	1.34 ± 0.09	2.29 ± 0.15
—	—	—	−133	2.15 ± 0.38	4.47 ± 0.79	−127	1.46 ± 0.09	2.5 ± 0.15

The data listed are the I_m ± SD measured and the I_m normalized to I_m at zero membrane potential (n = 18–24 for each datum).

membrane potentials for each set of conditions. And Fig. 1 shows the I_m measured as a function of the membrane potential under 50 mM trans Na^+ conditions. Note that the I_m increases with hyperpolarization for all three sets of data as illustrated in Fig. 2, indicating that at least one step in the transport process is potential dependent and is either rate limiting itself, or its potential dependence alters the fraction (density) of carrier in a conformation involved in a rate-limiting transition. As expected, the absolute value for I_m at saturating Na_o^+ was consistently greater than the I_m measured under the other two conditions.

To determine the loci of potential dependence of the transport mechanism, one must observe the relative rate of change in I_m as a function of changes in membrane potential under the different solute conditions (Bennett and Kimmich, 1992). To accomplish this comparison, the I_m data for each set of conditions were normalized by setting the value obtained at zero potential to 1.0 and expressing all other I_m values for the same solute concentrations as a multiple (or fraction) of the zero potential value. Fig. 3 graphs these normalized I_m as a function of membrane potential for all three solute conditions. This graph therefore indicates the rate of change in I_m as a function of the membrane potential. Table 1 lists the normalized I_m ± SD for each set of sodium conditions at all tested membrane potentials. Note that the relative rate of change in I_m is different for the two different extracellular Na^+ concentrations with zero trans Na^+. When 50 mM trans Na^+ is present, the rate of I_m increase mimics that observed for the zero trans case with saturating extracellular Na^+. The significance of these potential-dependent characteristics of cotransporter kinetics was examined further through analysis of appropriate models of reaction schemes for the transport cycle to evaluate their implications regarding transport mechanism.

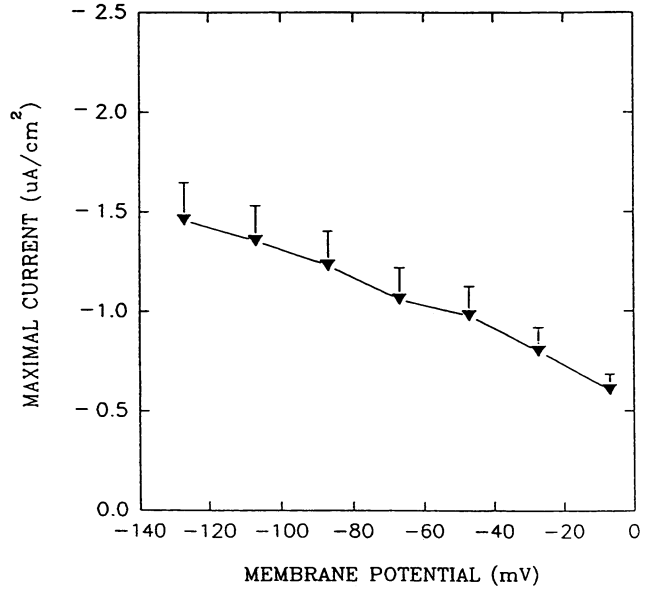

FIGURE 1 Maximal current as a function of membrane potential under saturating external sodium and 50 mM trans sodium conditions. Points are the I_m ± SD. The line is not theoretical. The internal solution contained 50 mM sodium and zero AMG.

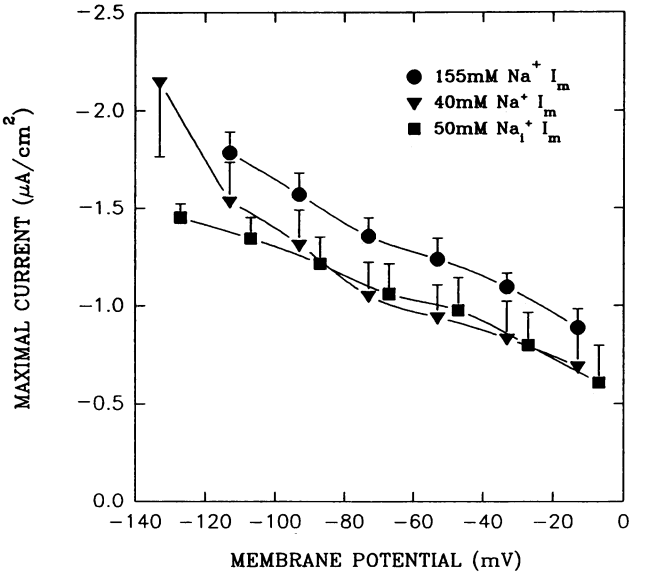

FIGURE 2 Maximal current as a function of membrane potential for all three solute conditions. The absolute values of the maximum current as a function of membrane potential. Points are I_m ± SD at a membrane potential. Lines are not theoretical.

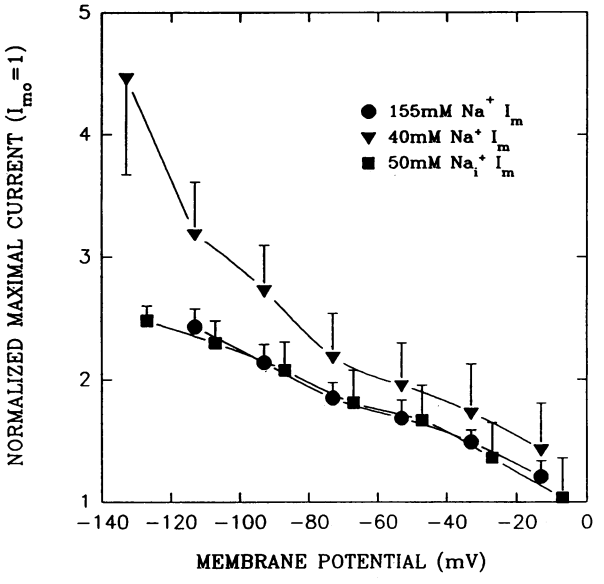

FIGURE 3 Normalized maximal current as a function of membrane potential. Points are the data normalized to the value at zero membrane potential ± SD. Lines are not theoretical.

Development of a model

The following analysis evaluates the validity of various models in which the loci selected for rate limitation and potential dependence are varied by comparing the results predicted by the models with the experimental relationships observed for the kinetics and potential dependence of Na^+/sugar cotransporter activity. King-Altman methods (King and Altman, 1956; Segel, 1975; Hill, 1977) were used to solve the differential equations describing carrier pool densities (see Appendix). From these relationships, the equation describing I_m (Appendix, Eq. 9) was used to calculate I_m for a given model and to predict the effect of changes in membrane potential on I_m under the various solute conditions that were tested. The plausibility of a particular model is tested by evaluating how well the magnitude of change in maximal transport activity observed experimentally agrees with that predicted algebraically as solute levels are changed. Using this approach, it can be shown that many models do not adequately account for the measured data.

The analysis shows that the magnitude of potential dependence of I_m under 155 mM Na_o^+ conditions requires that at least one of the rate-limiting steps in the cycle must be potential dependent. Otherwise, increases in I_m with membrane potential could not be as dramatic as those measured. Electroneutral sugar binding/dissociation events are presumed to be unlikely sites for potential dependence of the cycle. Limitation of possible rate-limiting steps is provided by the transinhibition data, which show that the potential dependence of I_m at saturating extracellular Na^+ is not dependent on internal Na^+ levels (the magnitude of increase in I_m with membrane potential for 155 mM Na_o^+ is identical for zero and 50 mM trans Na^+ (see Tables 1 and 2 and Fig. 3). Furthermore, the absolute value of I_m is lower when Na^+ is present on the trans side of the membrane. Taken together, these data indicate that internal Na^+ binding/dissociation events are not potential dependent. Therefore, internal Na^+ binding events cannot be the sole rate-limiting step(s). External Na^+ binding events are not likely to be rate limiting, at least at high external Na^+, because I_{AMG} at 155 mM Na^+ is between 91% and 94% saturated at all tested membrane potentials (Bennett and Kimmich, 1992). If the binding and/or dissociation of Na^+ were rate limiting, then the degree of saturation of the binding site by external Na^+ should show a pronounced potential dependence, contrary to the experimental evidence. Therefore, these events cannot be the sole rate-limiting step(s).

TABLE 2 Parameters measured and the range of values acceptable under each of the three solute conditions tested

Solute condition	I_{mr}	Acceptable I_{mr}	Fold-increase in I_m	Acceptable fold-increase in I_m
155 Na_o^+	1.0	1.0	2.4	>2.0
40 Na_o^+	1.53	1.2–2.0	4.4	>3.0
50 Na_i^+	1.25	1.0–1.5	2.5	2.0–3.0

The ratio of I_{mo} at 155 Na_o^+ versus I_{mo} at 40 Na_o^+ and 50 Na_i^+ is listed as I_{mr}. The values of I_{mr} that are considered a reasonable match for the models tested follow. The increase in I_m over the range of potentials tested and the level of this increase that is considered acceptable to a given model are also listed.

The only remaining possible rate-limiting events are the conformational changes or "translocation" events of the free and fully loaded carriers. For any cotransport system, changes in protein conformation are necessary to allow binding and release of substrate at opposite sides of the membrane. It is intuitively satisfying to predict that the slow transition of cotransport mechanisms might be due to conformational changes in a macromolecule embedded in the membrane matrix rather than to solute diffusion events. This intuitive expectation is reinforced by numerous observations showing that the rate of ion transfer via cotransport systems (i.e., turnover number) is at least five orders of magnitude slower than that found for transfer through ion channels where pronounced macromolecular conformational changes are not necessary (Kimmich, 1990). The approach presented below begins with analysis of models in which conformational events are assigned rate limitation and works toward examination of predictions derived from situations in which other sites in the transport cycle are assumed to be rate limiting in an attempt to identify all plausible models of cotransport kinetics that fit the observed data.

Description of the model

Fig. 4 illustrates an eight-state reversible model for a 2:1 Na^+/glucose (AMG) cotransporter as previously described by Restrepo and Kimmich (1985a,b, 1986). This model differs from that presented by Parent et al. (1992b) in two significant ways: 1) the binding of each Na^+ is considered

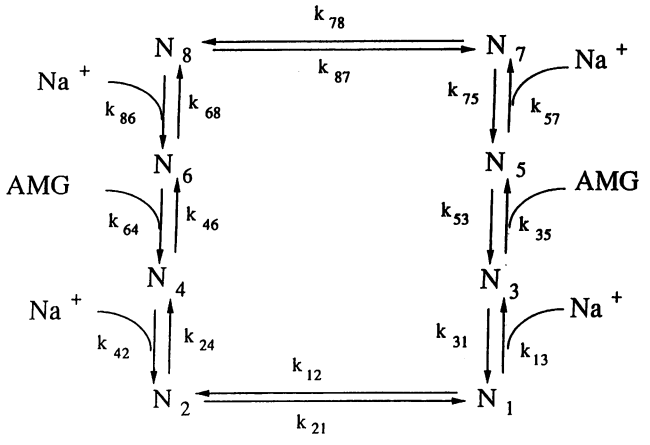

FIGURE 4 Model describing a 2:1 Na^+/glucose sequential and fully reversible transport mechanism. The figure depicts eight carrier states (denoted N1–N8) and rate constants signifying the rate of transition from one carrier state to the next (e.g., the transition from N1 to N2 is characterized by the rate constants k_{12}). The binding and dissociation of solutes are noted accordingly.

an independent event in our model, and 2) the "slippage" event described by Parent is not included. Because there is ample evidence for differing characteristics governing the binding of each sodium ion to its site, as described earlier, we believe our model more closely represents actual molecular events in the transport cycle. The lack of "slippage" in our model is due to the fact that we see no experimental evidence indicating slippage in native transport systems for either intestinal or renal tissue, as previously described (Kimmich and Randles, 1984, 1988; Smith-Maxwell et al., 1990; Bennett and Kimmich, 1992). In part, this is indicated by the fact that the Hill coefficient at various external sodium levels remains constant, which is not expected if there is flow of sodium in the absence of sugar. Moreover, the addition of phlorizin to a sugar-free medium does not diminish whole-cell currents in LLC-PK_1 cells, even though subsequently added sugar can no longer induce a current (Smith-Maxwell et al., 1990). This is in contrast to the case with the oocyte expression system, where phlorizin-sensitive currents can be seen in the absence of added sugar (Umbach et al., 1990).

In the model chosen for evaluation, 16 rate constants (shown as k_{xy}, where x is the carrier pool from which the transition begins, and y is the carrier pool to which the transition ends) are necessary to completely describe the system. Rate constants are in units of inverse time. The rate constants that pertain to solute-binding events are multiplied by the concentration of the solute that is binding. These "composite" rate constants will be referred to as rate constants, although it should be recognized that they are the product of a rate constant and the applicable solute concentration for that step in the cycle.

Steady-state kinetics are assumed, and therefore, all carrier pool densities remain constant over time. The methods of King and Altman (King and Altman, 1956; Segel, 1975; Hill, 1977) were used to solve the differential equations describing the carrier pool densities. The diagrams used to solve the differential equations are shown in the Appendix. Also included is the algebra involved in transforming the general rate equation to a form similar to that of the Michaelis-Menten equation. From this equation, the equations for K_m (Appendix, Eq. 10) and I_m (Appendix, Eq. 9) can be determined. A computer program for the generic model and corresponding equations for solute K_m and V_{max} (I_m) was written to facilitate calculations. This program calculates I_m and K_m for a given set of rate constants and was used to evaluate the plausibility of the various models described below.

Assumptions used for all fitting procedures are as follows: 1) steady-state kinetics are assumed throughout; 2) all rate constants at high external Na^+ concentrations other than the rate-limiting constant(s) are at least 10-fold greater than the rate-limiting rate and are equivalent; and 3) binding rates for internal solutes are assumed to be zero under zero trans conditions.

Data comparing I_m as a function of membrane potential were extrapolated to zero membrane potential (I_{mo}) by assuming that the I-V relationship is sigmoidal in nature and fitting the data to the following equation:

$$I_m = I_{ma}/[1 + \{\exp(u - b)/k\}],$$

where I_{ma} is the absolute maximum current, u is the membrane potential, b is the membrane potential at half-maximum current, and k is the slope factor describing the curve. Sigmoidicity of the current-voltage relationship is implied because activity of the transport protein will saturate at both the inward-transporting (negative current) and outward-transporting (positive current) ends of the voltage axis. The rate of the steps that are not rate limiting relative to the rate-limiting step(s) is determined using I_{mo} calculated under the two zero trans experiments (155 mM and 40 mM external Na^+ concentrations). The Na^+ binding rate at 40 mM Na^+ must decrease fourfold from the rate of binding at 155 mM Na^+ because of the aforementioned concentration effects on rates of solute-binding events. One can establish the magnitude of the rate constants relative to the rate-limiting rate necessary to attain the 1.53-fold increase in I_{mo} observed experimentally for a fourfold increase in external Na^+ concentration. This ratio of I_{mo} at 155 Na_o^+ to I_{mo} at 40 Na_o^+ is called $I_{mr}(40)$. If a model is plausible, a set of rate constants that gives a value near the measured $I_{mr}(40)$ must be definable. Furthermore, the models must predict increases in I_m with hyperpolarization consistent with the measured increases. Table 2 lists the I_{mr} and the increase in I_m over the range of membrane potentials tested for each set of data and lists the range of these parameter values that were acceptable in this analysis. For example, $I_{mr}(40)$ within a range of 1.2 to 2.0 was considered sufficient to warrant further evaluation of a particular model ($I_{mr}(40)$ = 1.53). Rate constants for steps in a given model other than the rate-limiting step were set at values 10, 100, and 1000 times the rate of the rate-limiting step in different trials, and

the predicted $I_{mr}(40)$ was calculated. If $I_{mr}(40)$ fell within the 1.2–2.0 range for any trial, the optimum relative rates for constants applying to steps that are not rate limiting were determined through iteration of the magnitude of those rates to improve the fit to $I_{mr}(40)$.

When rates for the Na^+ binding steps relative to the rate-limiting step had been chosen by this procedure, predictions of the potential dependence of the system were made using the data collected. First, a fit of the data to a particular potential-dependent scheme was made for the 155 Na_o^+ data. All potential dependent transitions were assumed to follow Eyring rate theory (Eyring et al., 1949; Woodbury, 1971). A plausible scheme was defined as one that predicts at least a twofold increase in I_m as the potential is changed from 0 to −113 mV (see Table 2). Models predicting plausible fits at 155 Na_o^+ were then used to calculate I_m at 40 Na_o^+. Plausible models will show at least a threefold increase in I_m from 0 to −133 mV. The measured potential-dependent effect at 40 Na_o^+ was 4.4-fold, but a minimum of a threefold increase was used to ensure that all plausible models were tested. However, if an optimized model still shows only a threefold increase in I_m at 40 Na_o^+, then it was not considered to be an accurate means of describing the transport mechanism. All models for which calculations are not shown do not meet the criteria described above. Models that meet these three basic criteria ($I_{mr}(40)$ = 1.2–2.0, and I_m increases with membrane potential as listed in Table 2) were tested further in an attempt to attain a better fit to the data.

Iteration of the potential dependence of the system for a plausible model was made in an attempt to achieve a predicted I_m that is optimally consistent with the measured data. When a plausible model meets these more stringent requirements (often beforehand), the transinhibition data were used to verify further the plausibility of the model. Again, the change in I_{mo} with addition of internal Na^+ ($I_{mr}(50)$ = 1.25) can be used to calculate what the internal Na^+ association rates must be relative to the rate-limiting step. This value was used to calculate the predicted I_m as a function of membrane potential. Models yielding a minimum of a twofold increase in I_m over the range 0 to −127 mV and a maximum of a threefold increase in I_m were considered further. Again, optimum fitting of the potential dependence data under this set of conditions was made in an attempt to fit all of the data within the measured standard deviations. Any model meeting the above, less stringent criteria (i.e., a two- to threefold increase in I_m over the range of tested membrane potentials) was studied further to optimize the potential-dependent scheme for that model. Models that did not meet the less stringent criteria were dismissed as implausible.

Models tested

Translocation of the free carrier is the sole rate-limiting step

All previous efforts to model the transporter have assumed that free carrier translocation is rate limiting (Aronson, 1978; Kessler and Semenza, 1983; Sanders et al., 1984; Restrepo and Kimmich, 1985a,b, 1986; Bennett and Kimmich, 1992; Parent et al., 1992b). This assumption was based largely on intuitive reasoning that the rates of conformational changes in macromolecular transport proteins embedded in the membrane matrix probably are much slower than the rate of solute binding and dissociation events. For these reasons, our initial modeling also assumed that translocation of the free carrier is the sole rate-limiting step of the transport cycle.

Best fits for this case occur when rates at which Na^+ binds at high external levels (155 mM) are 16 times the rate of the rate-limiting step, slowing to only four times the rate-limiting step at 40 mM external Na^+. These assigned rates give a value for $I_{mr}(40)$ = 1.58, consistent with the 1.53 measured ratio. However, potential-dependent translocation of free carrier translocation cannot by itself account for the increased potential dependence of I_m at low Na^+, because I_m at 40 Na_o^+ is then predicted to show a much less dramatic potential dependence than I_m at 155 Na_o^+, in contrast to the observed relationship. Furthermore, even by assuming that the two external Na^+ sites are maximally potential dependent (i.e., that each Na^+ ion "senses" the full electric field in reaching its binding site), there is not a sufficient increase in I_m. For this situation, I_m at 155 Na_o^+ is predicted to increase only 1.24-fold over the 113 mV range tested. If the two internal Na^+ dissociation events are assumed to be maximally potential dependent, the predicted increase in I_m for both 40 Na_o^+ and 155 Na_o^+ is too low (1.18-fold for I_m at 155 Na_o^+, and 1.21-fold at 40 Na_o^+). Maximum potential dependence for dissociation of internal Na^+ in combination with potential-dependent free carrier translocation also does not give a good fit to the data, because I_m at 40 Na_o^+ would increase only 2.17-fold under these conditions. Finally, potential dependence for translocation of free and fully loaded carrier forms does not account for the increase in the potential dependence of I_m at the lower external Na^+ level (I_m at 40 Na_o^+ increases only 2.47-fold).

Only two plausible models were found under the starting assumption that free carrier translocation is solely rate limiting. In both cases, sodium-binding events as well as free carrier translocation must be potential dependent. Free carrier translocation must be potential dependent to account for the potential dependence of I_m with saturating Na^+ levels, whereas potential-dependent Na^+ binding is necessary to explain the increased potential dependence of I_m at lower external Na^+ levels. The zero trans Na^+ data can be described well by assuming extracellular Na^+ binding and intracellular Na^+ dissociation events are all potential dependent. Fig. 5 *A* shows the measured data and the predicted curves under the assumption that all four Na^+ events and free carrier translocation are potential dependent. The field fraction for specific potential-dependent steps is given in the figure legend. Fig. 5 *B* shows the predicted curves assuming that only the two external Na^+ binding events

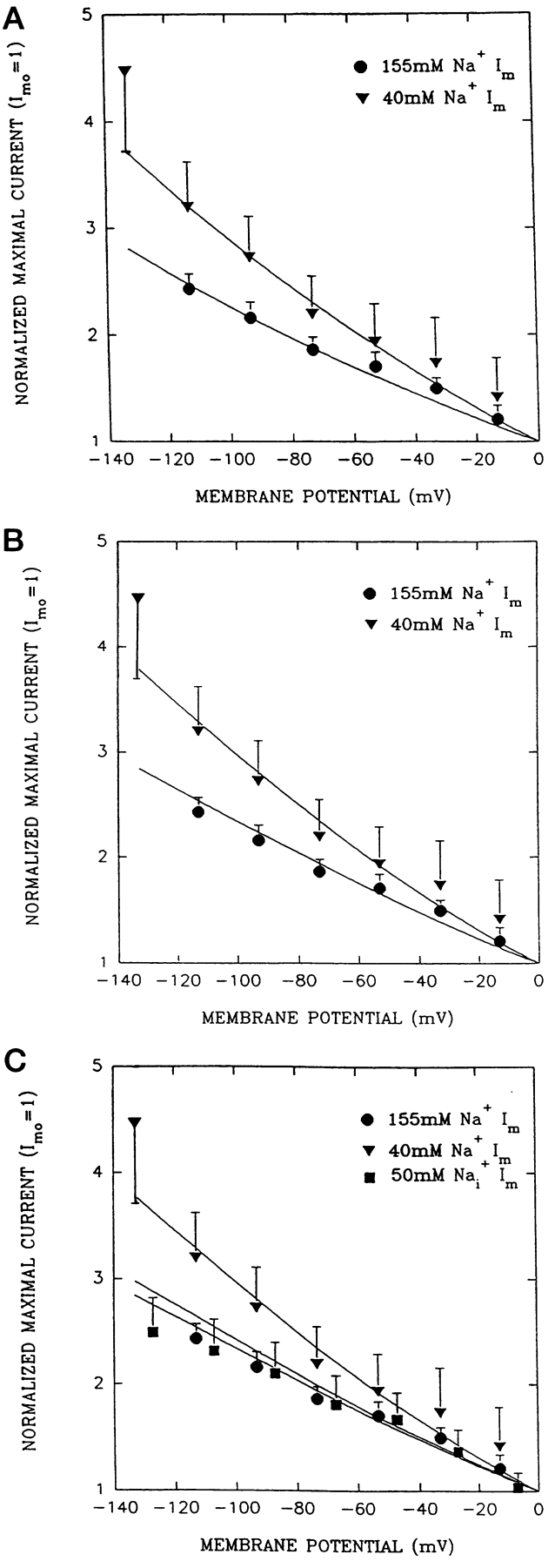

FIGURE 5 Normalized maximal current and the predicted values assuming translocation of the free carrier is the sole rate limiting event. (*A*) Predicted maximal current assuming that translocation and all four sodium binding events are potential dependent. Points are the normalized I_m ± SD as a function of membrane potential. The lines drawn are predictions of the model assuming all four sodium binding events as well as free carrier translocation are potential dependent. Eyring rate fits: $n = 0.2$ for k_{78}, k_{87}, k_{42}, k_{24}, and k_{13}; $n = 0.7$ for k_{86}, k_{68}, and k_{57}. Eyring rate theory was used for this and all other fits. The equation used to describe the rate constants is

$$k = k_0 \exp(-FnV/RT),$$

where k_0 is the inherent rate constant at zero membrane potential; F, R, and T are constants with their typical values; V is the membrane potential; and n is the fraction of the electric field utilized in the transition from one carrier state to the next. (*B*) Predicted maximal current assuming the two external sodium binding events as well as free carrier translocation are potential dependent. Points are the normalized I_m ± SD as a function of membrane potential. The lines drawn are predictions of the model assuming only the two external sodium binding events and free carrier translocation are potential dependent. Eyring rate fits: $n = 0.3$ for all six events (k_{78}, k_{87}, k_{86}, k_{68}, k_{42}, k_{24}). (*C*) Predicted maximal current for all three solute conditions. Adding the transinhibition data to the data in *B*.

and free carrier translocation are potential dependent. Again, the potential dependence of the individual rate constants is described in the figure legend.

Insight into the degree to which potential-dependent internal Na^+ dissociation events are necessary can be gained by looking at details of the transinhibition data. Because I_m as a function of membrane potential is nearly identical under zero trans and transinhibited conditions, it is unlikely that internal Na^+ events are potential dependent. If the rate constants describing the internal Na^+ events were significantly potential dependent, I_m under transinhibited conditions would increase much faster than the observed increase for zero trans Na^+. It does not, and therefore one of the two possible models described above is found to be insufficient. The only plausible model that fits all of the measured data is shown in Fig. 5 *C*, in which translocation of the free carrier and each of the two external Na^+ events are potential dependent.

Rate-limiting translocation of free carrier with inward translocation rate twice that of the outward rate

Evidence from two previous studies has indicated that the free carrier is predominantly inward facing at zero membrane potential (Kessler and Semenza, 1983; Restrepo and Kimmich, 1985b). Through kinetic analysis of potential dependent sugar influx, these studies have shown that approximately one-third of the total free carrier is in an outward-facing conformational state and about two-thirds is inward facing. This implies that, if free carrier translocation is the rate-limiting step, then inward translocation must be twice the rate of outward translocation.

When the rate of inward free carrier translocation is set at twice the rate of outward translocation, the optimum relative rate of the other steps in the cycle is 24, thereby giving an

$I_{mr}(40) = 1.51$. Only two plausible models were found given these conditions: 1) potential-dependent translocation of free carrier and maximal potential dependence of the second external Na^+ binding event, and 2) potential-dependent translocation and potential dependence of both external Na^+ events. As in the previous example, all combinations of potential-dependent events that gave reasonable fits were evaluated for optimum fitting. Fig. 6 *A* shows the predicted curves assuming that the second external Na^+ event is maximally potential dependent, and determining the best fit for potential-dependent free carrier translocation to the data for 155 mM Na_o^+ (the best fit resulted in translocation "sensing" 27% of the electric field). This model barely meets the criteria needed to be considered a plausible model because the increase in I_m under 40 Na_o^+ conditions is only 3.3-fold (compared to the 4.4-fold increase that was measured). There is no way of increasing the effect of the membrane potential on this system, given that the second Na^+ binding event was already assigned maximum potential dependence. Therefore, this model does not describe the potential dependence of the transporter in a totally satisfactory manner.

Fig. 6 *B* shows the predicted curves for the second possibility, in which free carrier translocation and both external Na^+ events are potential dependent. The fraction of field "sensed" by each potential-dependent event is given in the figure legend.

Calculating the predicted I_m under Na^+ transinhibited conditions using the model described in Fig. 6 *B* above results in predictions that are consistent with observation. Therefore, if free carrier translocation is the rate-limiting step of the transport cycle, then the only plausible potential-dependent scheme that describes all of the data gathered in this report is when translocation and both external Na^+ events are potential dependent. The relative potential dependences of the individual rates vary, depending on the relative magnitude of the rate constants, but the evidence under this assumed model indicates that all three steps must be potential dependent.

Rate-limiting translocation of the fully loaded carrier

Calculations were also made to determine the I_{mo} predicted for the two zero trans experiments (40 and 155 Na_o^+), assuming that fully loaded carrier translocation is rate limiting. For this case, the lowest possible value for $I_{mr}(40)$ is 2.3. Calculations were done for a wide range of rates for the non-rate-limiting steps (10- to 1000-fold faster than the rate-limiting rate) and assuming various relative rates for the inward and outward translocations of the solute-loaded cotransporter. A lower limit of 2.3 for $I_{mr}(40)$ is not acceptable relative to the experimentally observed value of 1.53. Therefore, models in which translocation of the loaded carrier is rate limiting are not considered plausible choices.

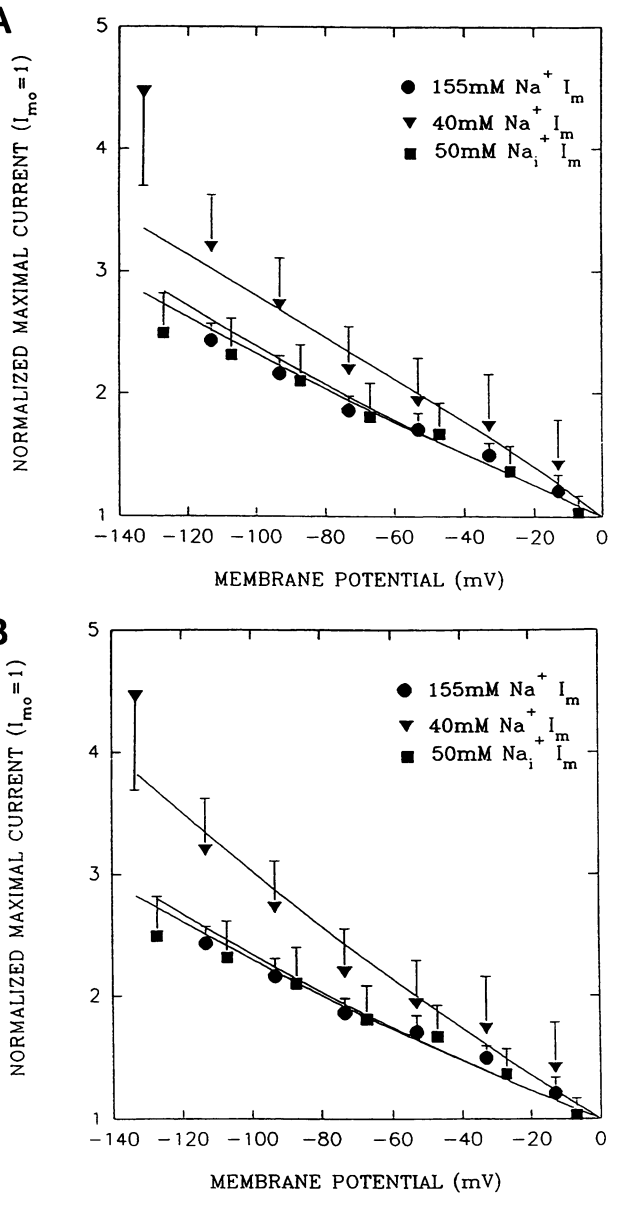

FIGURE 6 Predicted potential dependence of the maximal current, assuming rate-limiting free carrier translocation in which the inward rate is twice that of the outward rate. (*A*) Theoretical fits assuming that the second external sodium binding event is maximally potential dependent and that free carrier translocation is the only other potential dependent event. Points are the normalized $I_m \pm$ SD as a function of membrane potential. The lines drawn are predictions of the model with Eyring rate fits as follows: n = 0.27 for free carrier translocation (k78, k87); n = 1.0 for the second external binding events (k42, k24). (*B*) Theoretical fits assuming the two external binding events and free carrier translocation are potential dependent. Points are the normalized $I_m \pm$ SD as a function of membrane potential. The lines drawn are predictions of the model with Eyring rate fits as follows: n = 0.25 for free carrier translocation and the second external sodium binding event (k78, k87, k42, k24); n = 0.8 for the first external sodium binding events (k86, k68).

Both free and fully loaded carrier translocation are rate limiting

Calculations show that when all four translocation events are equivalently rate limiting, a suitable $I_{mr}(40)$ cannot be

calculated. An $I_{mr}(40)$ of 1.75 was calculated for the situation in which inward rates are twice the outward rates for both translocation events when both events are rate limiting. However, the potential dependence of I_m cannot be fit to observed values under these assumptions. Potential dependence of either or both translocation events also proved insufficient for acceptable fitting. To attain an $I_{mr}(40)$ as low as 1.75, all non-rate-limiting rate constants must be set to 1000 times that of translocation. Therefore, potential-dependent Na^+ binding events had little effect on I_m. Nor is it possible to achieve a good fit to the data assuming combinations of potential dependent events such as translocation of the free and fully loaded carrier in addition to the four Na^+ binding/dissociation events. Therefore, a model in which both translocation events are rate limiting cannot effectively describe the transport mechanism.

In summary, attempts were made to find plausible models assuming that translocation of the free and/or fully loaded carrier is rate limiting. Rate limiting translocation of the fully loaded transporter or the combination of rate limitation for translocation of both free and fully loaded carrier forms proved to be models that could not be fit well to the measured data. The only potential-dependent scheme that explains all of the data given the assumptions of this model is if both external Na^+ events and free carrier translocation are potential dependent, with free carrier translocation as the slow transition in the cycle.

This model fits all available data (see Figs. 5 *C* and 6 *B*) but is not conceptually complete. There must be an additional potential-dependent event to account for the lack of potential dependence of the internal Na^+ events. This is necessary because the best fitting occurs when Na^+ ions bind in a potential-dependent manner but do not cross the entire electric field. For the eight-state model discussed here, the additional potential-dependent event is fully loaded carrier translocation. This form of the carrier must change in conformation to allow the Na^+ ions access to the interior of the cell, and the conformational change must be potential dependent to account for the lack of potential dependence of internal Na^+ dissociation events. Taken together the evidence points toward a conformational change for the loaded carrier that shifts the position of the charge associated with the Na^+ ions with respect to the electric field. This change allows the ions to dissociate from the protein in a manner that is independent of the membrane potential. It is therefore likely that four potential-dependent events exist: binding/dissociation of the two Na^+ ions at the extracellular side of the membrane, and both cotransporter translocation events. Fig. 7 shows that curves predicted from the model using these assumptions fit the data well.

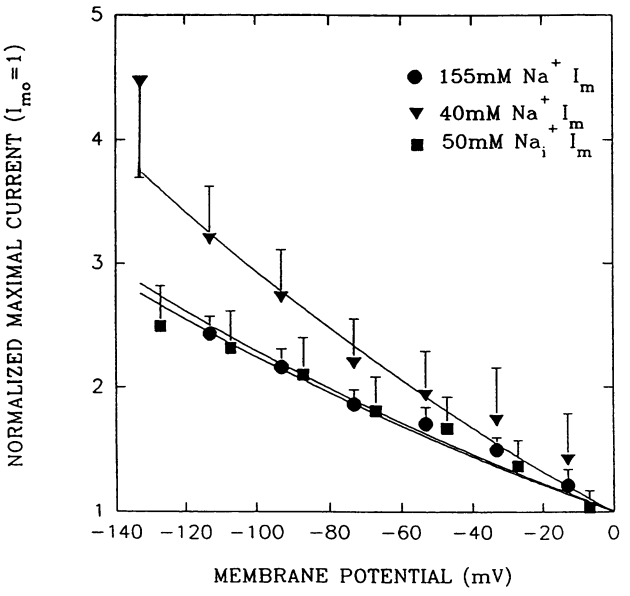

FIGURE 7 Model describing the potential dependence of the transporter (model 1). Free carrier translocation is rate limiting, with both translocation events and the two external sodium binding/dissociation events potential dependent. Points are the normalized I_m ± SD as a function of membrane potential. The lines drawn are predictions of the model with Eyring rate fits as follows: $n = 0.22$ for free carrier translocation (k78, k87); $n = 0.18$ for fully loaded carrier translocation (k21, k12); $n = 0.3$ for both external sodium binding events (k86, k68, k42, k24).

Is it possible for any other single step in the transport cycle to be rate limiting?

Each rate constant was tested for plausibility as a sole rate-limiting step using the methods outlined above. Under zero trans conditions, only 13 rate constants were considered because the three internal binding rates are assumed to be zero. Only two of the 13 proved to be plausible using the less stringent criteria listed earlier: 1) dissociation of the second-off internal Na^+ and 2) dissociation of AMG. Neither of these events can reasonably be considered the sole rate-limiting event for reasons discussed above. Therefore, no individual events other than translocation of free carrier prove to be satisfactory as sole rate-limiting steps.

Evidence for the necessity of rate-limiting free carrier translocation is quite compelling. However, it is also of interest whether any transport event in addition to carrier translocation might provide dual sites for rate limitation. All two-site combinations were evaluated, but as described below, only one model of this type was found to be plausible.

Free carrier translocation and the first internal Na^+ dissociation event are rate limiting (an example of an occluded Na^+ bound state)

In the search for all plausible models describing the transporter mechanism, one example (and only one) in which the extracellular Na^+ binding events are not required to be potential dependent was found (however, even in this case these events are not excluded from being potential dependent). If translocation of the free carrier and dissociation of the first-off internal Na^+ are both rate limiting, then the data can be fit well assuming that only free and fully loaded carrier translocations are potential dependent. Fig. 8 shows the quality of fit to the measured data for curves calculated

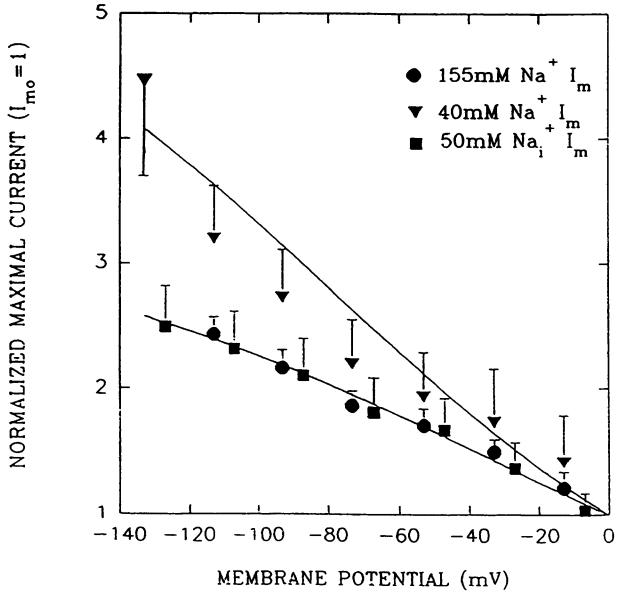

FIGURE 8 Second model describing the potential dependence of the transporter in which a sodium-occluded state exists (model 2). Free carrier translocation and the first internal sodium dissociation events are rate limiting. Only the two translocation events are potential dependent. Points are the normalized I_m ± SD as a function of membrane potential. The lines drawn are predictions of the model with Eyring rate fits as follows: n = 0.17 for free carrier translocation (k78, k87); n = 0.29 for fully loaded carrier translocation (k12, k21).

using these assumptions. The extent of potential dependence of each potential-dependent step is listed in the figure legend. Therefore, the above fitting procedure shows that when one removes the assumption that free carrier translocation is the sole rate-limiting event, then the possible potential-dependent loci of the system change.

DISCUSSION

The calculations described above are powerful in that they enable one to limit the possible potential-dependent and rate-limiting events that describe Na^+/glucose cotransporter activity. The need for rate-limiting free carrier translocation was described in detail and shown mathematically. If this is the only rate-limiting step in the transport cycle (i.e., if all other events are minimally ten times faster under saturating solute conditions), then both Na^+ binding events at the extracellular surface and both carrier translocation events must be potential dependent. When another equally slow step is included in the transport cycle (dissociation of the first internal Na^+), then a different basis for potential dependence in which only carrier translocation events need be potential dependent is also consistent with the experimental data, although potential-dependent Na^+ binding events can still be included as part of this model.

A model of the latter type is analogous to the occluded Na^+ state that Lauger has described for Na^+/K^+ ATPase (Lauger and Apell, 1988a,b). He envisioned that the Na^+ ion, after binding to the protein, cannot dissociate from the protein because a thermodynamic energy barrier precludes a transition to a conformational state that allows release to the macroscopic environment. The energy barrier diminishes the rate of dissociation of Na^+ from the inwardly facing carrier. Lauger found that this conceptual model can explain much of the potential dependence observed for ATPase activity. Recent studies measuring transient ATPase activity have confirmed that an occluded-like state of the protein indeed exists in which the last sodium to be released from its binding site is a slow step in the pathway (Gadsby et al., 1993; Hilgemann, 1994).

The two viable models raise an obvious new question: can it be determined whether bound Na^+ is held and released slowly from the protein, or is free carrier translocation the only slow event of the transport cycle? At the moment, direct evidence validating either model is not available. Nevertheless, certain facts relating to the effect of trans Na^+ on the system tend to favor the model in which free carrier translocation is the sole rate-limiting step. The most compelling of these pertain to observations by Kimmich and Randles (1984), who showed that elevated intracellular Na^+ causes a pronounced transinhibition of transporter function in ATP-depleted intestinal cells when the membrane potential is depolarized, as also shown here for renal cells. The Kimmich and Randles (1984) report showed that the transinhibition could be largely alleviated as the potential is repolarized to approximately 60 mV (interior negative), in contrast to our observations described above. However, the earlier data were gathered at low external AMG concentrations (0.1 mM), rather than at the relatively high concentration used in this study.

To assess whether either of the two plausible models discussed here can accommodate the observation of potential-dependent relief of transinhibition, we used each model to calculate the influence of trans Na^+ on transport rates at low (0 mV) or high (−60 mV) values of membrane potential under the conditions used by Kimmich and Randles (100 μM extracellular AMG; 135 mM extracellular Na^+; zero trans AMG). Both models correctly predict the inhibitory effect of 50 mM trans Na^+ at zero membrane potential. However, only the model in which translocation of the free carrier is solely rate limiting predicts the observed relief of transinhibition with increasing hyperpolarization of the membrane potential. This model predicts that the influx of sugar at 0 mV with trans Na^+ present will be only 60% of the influx under zero trans conditions, whereas the sugar influx at −60 mV with 50 mM trans Na^+ is 98% of that with zero trans Na^+. The occluded Na^+ model predicts that the membrane potential has virtually no effect on Na^+ transinhibition of sugar influx. That is, the model predicts little or no relief of transinhibition through hyperpolarization. Furthermore, the influx of sugar with high trans Na^+ at both membrane potentials is only 40% of the influx of sugar under zero trans conditions. These predictions conflict with the data presented by Kimmich and Randles (1984).

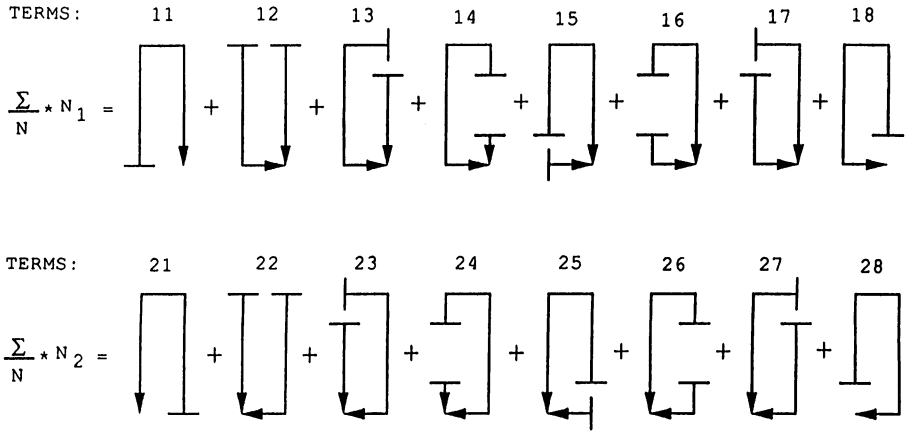

FIGURE 9 King-Altman diagrams determining carrier pool densities. Shown are the King-Altman diagrams drawn for two of the eight carrier pool density equations. The carrier states are outlined in Fig. 4. Each term is the product of the seven rate constants needed to reach the carrier pool in question and determined by the pathways defined in the figure. The solution of the differential equation describing each carrier pool density is the sum of all terms as indicated in the figure (there are a total of eight terms for each carrier state). The remaining six carrier pool densities are defined in the same manner.

In summary, we have tested the plausibility of many different models for Na^+/sugar cotransporter function based on the degree to which mathematical calculations derived from various possible models agree with the observed potential dependence for maximum rates of function of the cotransporter. Only two models prove to be plausible: 1) Translocation of the free carrier is rate limiting and potential dependent. Both external Na^+ binding events and translocation of the fully loaded carrier must also be potential dependent, or 2) Translocation of the free carrier and dissociation of the first internal Na^+ are rate-limiting events and both translocation events must be potential dependent. Evidence in favor of the first model exists, but it is rather indirect. Additional work is necessary before the validity of either model can be established with certainty.

APPENDIX

What follows is the quantitation of the kinetic model outlined in Fig. 4. Figure 9 illustrates the method used to solve the differential equations for two of the eight carrier pool densities. The other six densities were calculated similarly. Following this, the means of deriving the I_m and K_m for the transporter under steady-state conditions is shown.

Each term is the product of seven rate constants determined by multiplying the rate constants around the paths outlined in Fig. 9 (e.g., term 11 is $k_{24}k_{46}k_{68}k_{86}k_{75}k_{53}k_{31}$). Each carrier pool density is the sum of eight terms (e.g., $(\Sigma/N)^*N_1$ = terms 11 + 12 + 13 + 14 + 15 + 16 + 17 + 18).

Diagrams as drawn in Fig. 9 were drawn for each of the remaining six carrier states and were used to calculate the density of each carrier pool.

$$N = N_1 + N_2 + N_3 + N_4 + N_5 + N_6 + N_7 + N_8. \quad (1)$$

Σ is the sum of the equations describing all eight carrier pool densities:

$$\Sigma = (N_1/N) + (N_2/N) + (N_3/N) + (N_4/N) + (N_5/N) + (N_6/N) + (N_7/N) + (N_8/N). \quad (2)$$

The rate at which the transport functions can be determined as follows:

$$\text{Velocity } (v) = N^*(k_{21}N_2 - k_{12}N_1). \quad (3)$$

Canceling terms, all but terms 11 and 21 from Fig. 9 cancel, leaving

$$v/N = (k_{21}k_{13}k_{35}k_{57}k_{78}k_{86}k_{64}k_{42} - k_{12}k_{24}k_{46}k_{68}k_{87}k_{75}k_{53}k_{31})/\Sigma. \quad (4)$$

Internal AMG concentration in all experiments is nominally zero, therefore $k_{53} = 0$, and

$$v/N = (k_{21}k_{13}k_{35}k_{57}k_{78}k_{86}k_{64}k_{42})/\Sigma. \quad (5)$$

Σ can be separated into two groups, those terms containing k_{64} ($k_{64} = k_{064}{}^*S$), and those not containing k_{64}. As such,

$$\Sigma = \Sigma_0 + k_{064}S\Sigma_s, \quad (6)$$

where Σ_0 is the sum of all terms not containing k_{64}, and Σ_S is the sum of all terms containing k_{64}.

Therefore,

$$v/N = (Sk_{064}\,k_{21}k_{13}k_{35}k_{57}k_{78}k_{86}k_{42})/(\Sigma_0 + k_{064}S\Sigma_s). \quad (7)$$

Dividing Eq. 7 by $k_{064}\Sigma_S/k_{064}\Sigma_S$,

$$v/N = ((k_{21}k_{13}k_{35}k_{57}k_{78}k_{86}k_{42})^*S/\Sigma_s)/((\Sigma_0/k_{064}\Sigma_s) + S). \quad (8)$$

Rearranging Eq. 8 into the Michaelis-Menten form of $v = I_m{}^*s/K_m + S$ gives

$$I_m = (k_{21}k_{13}k_{35}k_{57}k_{78}k_{86}k_{42})/\Sigma_s, \quad (9)$$

$$K_m = \Sigma_0/k_{064}\Sigma_s. \quad (10)$$

The authors would like to thank Joan Randles for her advice and support throughout this work.

This work was supported in part by National Institutes of Health grant DD-15365.

REFERENCES

Aronson, P. S. 1978. Energy-dependence of phlorizin binding to isolated renal microvillus membranes. *J. Membr. Biol.* 42:81–98.

Bennett, E., and G. A. Kimmich. 1992. Na^+ binding to the Na^+-glucose cotransporter is potential dependent. *Am. J. Physiol.* 262:C510–C516.

Eyring, H., R. Lumry, and J. W. Woodbury. 1949. Some applications of modern rate theory to physiological systems. *Recent Chem. Prog.* 10: 100–114.

Gadsby, D. C., R. F. Rakowski, and P. DeWeer. 1993. Extracellular access to the Na, K pump: pathway similar to ion channel. *Science.* 260: 100–103.

Hamill, O. P., A. Marti, E. Neher, B. Sakmann, and F. J. Sigworth. 1981. Improved patch-clamp techniques for high-resolution current recording from cells, and cell-free membrane patches. *Pfluegers Arch.* 391: 85–100.

Hansen, U. P., D. Gradmann, D. Sanders, and C. L. Slayman. 1981. Interpretation of current-voltage relationships for "active" ion transport systems. I. Steady-state reaction-kinetic analysis of class-I mechanisms. *J. Membr. Biol.* 63:165–190.

Heinz, E., and P. Geck. 1978. The electrical potential difference as a driving force in Na^+-linked cotransport of organic solutes. *In* Membrane Transport Processes, Vol. 1. J. F. Hoffman, editor. Raven Press, New York. 13–30.

Hilgemann, D. W. 1994. Channel-like function of the Na/K pump probed at microsecond resolution in giant membrane patches. *Science.* 263: 1429–1431.

Hill, T. L. 1977. Free Energy Transduction in Biology. Academic, New York.

Hille, B. 1984. Ionic Channels of Excitable Membranes. Sinauer Associates, Sunderland, MA.

Kessler, M., and G. Semenza. 1983. The small-intestinal Na^+, D-glucose cotransporter: an assymetric gated channel (or pore) responsive to the membrane potential. *J. Membr. Biol.* 76:27–56.

Kimmich, G. A. 1990. Membrane potentials, and the mechanism of intestinal Na^+-dependent sugar transport. *J. Membr. Biol.* 114:1–27.

Kimmich, G. A., and J. Randles. 1980. Evidence of an intestinal Na^+:sugar transport coupling stoichiometry of 2.0. *Biochim. Biophys. Acta.* 596: 439–444.

Kimmich, G. A., and J. Randles. 1984. Sodium-sugar stoichiometry in chick intestinal cells. *Am. J. Physiol.* 247(*Cell Physiol.* 16):C74–C82.

Kimmich, G. A., and J. Randles. 1988. Na^+-coupled sugar transport: membrane potential-dependent K_m, and K_i for Na^+. *Am. J. Physiol.* 255(*Cell Physiol.* 24):C486–C494.

King, E. L., and C. Altman. 1956. A schematic method of deriving the rate laws from enzyme-catalyzed reactions. *J. Phys. Chem.* 60:1375–1378.

Lauger, P., and H-J. Apell. 1988a. Transient behavior of the Na^+/K^+ pump: microscopic analysis of nonstationary ion-translocation. *Biochim. Biophys. Acta.* 944:451–464.

Lauger, P., and H-J. Apell. 1988b. Voltage-dependence of partial reactions of the Na^+/K^+ pump: predictions of microscopic models. *Biochim. Biophys. Acta.* 945:1–10.

Parent, L., S. Supplisson, D. D. F. Loo, and E. M. Wright. 1992a. Electrogenic properties of the cloned Na^+/glucose cotransporter. I. Voltage-clamp studies. *J. Membr. Biol.* 125:49–62.

Parent, L., S. Supplisson, D. D. F. Loo, and E. M. Wright. 1992b. Electrogenic properties of the cloned Na^+/glucose cotransporter. II. A transport model under nonrapid equilibrium conditions. *J. Membr. Biol.* 125:63–79.

Restrepo, D., and G. A. Kimmich. 1985a. Kinetic analysis of mechanism of intestinal Na^+-dependent sugar transport. *Am. J. Physiol.* 248(*Cell Physiol.* 17):C498–C509.

Restrepo, D., and G. A. Kimmich. 1985b. The mechanistic nature of the membrane potential dependence of sodium-sugar cotransport in small intestine. *J. Membr. Biol.* 87:159–172.

Restrepo, D., and G. A. Kimmich. 1986. Phlorizin binding to isolated enterocytes: membrane potential, and sodium dependence. *J. Membr. Biol.* 89:269–280.

Samarzija, I., and E. Fromter. 1982. Electrophysiological analysis of rat renal sugar, and amino acid transport. V. Acidic amino acids. *Pflugers Arch.* 393:215–221.

Sanders, D., U. P. Hansen, D. Gradmann, and C. L. Slayman. 1984. Generalized kinetic analysis of ion-driven cotransport systems: a unified interpretation of selective ionic effects on Michaelis parameters. *J. Membr. Biol.* 77:123–152.

Segel, I. H. 1975. Enzyme Kinetics. Wiley, New York.

Smith-Maxwell, C., E. Bennett, J. Randles, and G. A. Kimmich. 1990. Whole cell recording of sugar-induced currents in LLC-PK_1 cells. *Am. J. Physiol.* 258(*Cell Physiol.* 27):C234–C242.

Umbach, J. A., M. J. Coady, and E. M. Wright. 1990. Intestinal Na^+/glucose cotransporter expressed in *Xenopus* oocytes is electrogenic. *Biophys. J.* 57:1217–1224.

Woodbury, J. W. 1971. Eyring rate theory model of the current-voltage relationship of ion channels in excitable membranes. *In* Chemical Dynamics: Papers in Honor of Henry Eyring. J. O. Hirschfelder, editor. John Wiley, New York. 601–617.